이학석사 학위논문

Controlling Cyclopolymerization using additive & Solvent aging experiment of *In-situ* Nanoparticlization of conjugated polymer

첨가물을 이용한 고리중합의 조절과 중합 도중 형성되는 공핵고분자의 자기조립체 연구

2014 년 8 월

서울대학교 대학원

화학부 유기화학전공

유 소 영

Controlling Cyclopolymerization using additive & Solvent aging experiment of *In-situ* Nanoparticlization of conjugated polymer

지도 교수 최 태 림

이 논문을 이학석사 학위논문으로 제출함
2014 년 6 월

서울대학교 대학원
화학부 유기화학전공
유 소 영

유소영의 이학석사 학위논문을 인준함
2014 년 6 월

위 원 장 _____ (인)

부위원장 _____ (인)

위 원 _____ (인)

Abstract

Controlling Cyclopolymerization using additive & Solvent aging experiment of *In-situ* Nanoparticlization of conjugated polymer

So Young Yu

Department of Chemistry,

The Graduate School, Seoul National University

First study is about controlling Cyclopolymerization.(CP) Cyclopolymerization of 1,6-heptadiyne derivatives using the Grubbs catalysts have been known to afford conjugated polyenes in low yields in dichloromethane (DCM), the most common solvent for olefin metathesis polymerization and a good solvent for typical conjugated polymers. Based on our previous work that showed highly efficient CP using the Grubbs catalysts in tetrahydrofuran (THF), we developed a new polymerization system using weakly coordinating additives with the third-generation Grubbs catalyst in DCM. The polymerization efficiency of various monomers and their controls dramatically increased by adding

3,5-dichloropyridine, yielding polymers with narrow polydispersity indices (PDIs) at low temperatures. These new reaction conditions not only expand the monomer scope by resolving the solubility concerns of conjugated polymers but also more effectively reduced the chain transfer. Consequently, fully conjugated diblock copolymer was successfully prepared.

Second study is about Solvent aging experiment of *in-situ* Nanoparticlization of conjugated polymer. (INCP)

There were many efforts to understand and mimic the natural structures using amphiphilic block copolymers. However, there were lots of works to induce self-assembly after synthesizing block copolymers such as annealing, dialysis and so on.

In our previous study, we found out *in-situ* formation of supramolecules when we used Meldrum's acid substituted monomer as 2nd block. We thought these self-assemblies were induced because of not only insolubility but also strong $\pi-\pi$ interaction of conjugated backbone of second block. Shapes of resulting nanoparticles were changed from single spherical core-shell structures to worm-like and aggregated micelles by adjusting the first and second block ratio.

Furthermore, we noticed that these structural changes also

occurred by solvent aging process. It was possible because block or gradient copolymer containing Meldrum's acid substituted CPs has high stability for solvents and additional chance to isoemrization. So, we studied about the conformational changes of nanoparticles synthesized *in-situ* manner using atomic force microscopy (AFM), Transmission electron microscopy (TEM), dynamic laser light scattering (DLS), and UV/Vis spectrum and so on.

Keywords : Cyclopolymerization, Coordinating effect, Self-assembly, solvent-aging process

Student Number : 2012-23041

Content

Part 1 :
Controlling cyclopolymerization in dichloromethane using additives which gives coordinating effect

1.1 Introduction

Cyclopolymerization (CP) of 1,6-heptadiyne derivatives via olefin metathesis provides a powerful and easy method for the synthesis of conjugated polyenes, whose utility has only increased with recent developments in CP living polymerization.[1] Early studies of CP were carried out using classical ill-defined catalysts, including Ziegler-Natta,[2-5] $MoCl_5$, and WCl_6, and thus provided little understanding of the CP mechanism.[6-11] However, recent work by Schrock and colleagues using well-defined Schrock catalysts has provided a better understanding of the mechanism of CP by examining the effects of catalyst regioselectivity on the structure of the polymer backbone.[12-16] Unfortunately, the common Ru-based Grubbs catalysts have not been effective in catalyzing CP, despite their utility in other olefin metathesis reactions.[17] Because the reactivity of Ru-carbenes for alkyne polymerization was much lower than that of Mo- or W-based catalysts,[18] Buchmeiser group replaced the X-type ligands on the Grubbs catalysts with stronger electron-withdrawing groups, obtaining greater reactivity for CP and, notably, regioselective control through exclusive α-addition (Scheme 1-1).[17,19-23] However, the modified initiators mostly showed low k_i/k_p values, making it difficult to prepare conjugated polyenes with low polydispersity indices (PDIs).

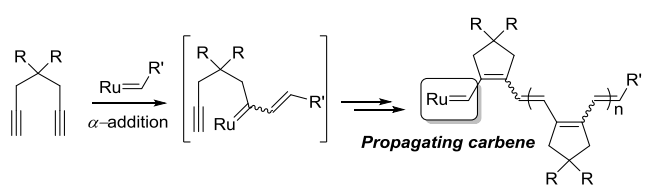

Scheme 1-1. Cyclopolymerization of 1,6-heptadiyne derivatives by Grubbs catalyst

Recently, we reported greatly enhanced reactivity in the CP of 1,6-heptadiyne derivatives using the third-generation Grubbs

catalyst[24] and the second-generation Hoveyda-Grubbs catalyst[25] that resulted from changing the solvent from dichloromethane (DCM) to tetrahydrofuran (THF). This discovery greatly expanded the utility of CP because the Grubbs catalysts not only promoted living polymerization of 1,6-heptadiyne[24] and 1,7-octadiyne derivatives via exclusive α-addition to afford conjugated polymers with narrow PDIs,[26,27] but also allowed for the preparation of block copolymers, rod-like molecular wires,[24,25] and nanospheres via direct self-assembly.[28] Despite the advantages of using THF, DCM is still a preferred solvent for CP, because conjugated polymers are generally much more soluble in chlorinated solvents. For example, diethyl dipropargylmalonate (DEDPM), which is one of the mostly used monomers for the CP, gives polymer that is insoluble in THF. Therefore, the utility and monomer scope of CP would be further broadened if conditions could be developed to achieve living polymerization in DCM.

In the previous report, we proposed that weakly coordinating THF effectively stabilizes the active propagating Ru carbene,[24] suggesting that detailed mechanistic investigations to understand the difference between THF and DCM would be valuable in expanding the utility of CP. Herein we report a new method of efficient living CP using the third-generation Grubbs catalyst in DCM by introducing weakly coordinating reagents as an additive, increasing the CP efficiency for various monomers to afford polyenes with controlled molecular weights and narrow PDIs that had previously been insoluble in THF. Furthermore, we demonstrate how the additive affect the lifetime of the active propagating carbene on the growing polymer chain end

1.2 Experimental

1.2.1 General experimental

All reactions were carried out under dry argon 9atmosphere using standard Schlenk-line techniques. Solvents for monomer synthesis were commercially obtained. For polymerization, dichloromethane (DCM) from Glass Contour Organic Solvent purification system was used. DCM was degassed for 10 minutes before using on polymerization. 1H NMR and 13C NMR were recorded by Varian/Oxford As-500 (500 MHz for 1H and 125 MHz for 13C) spectrometer and Agilent 400-MR (400 MHz for 1H and 100 MHz for 13C). Gel permeation chromatography(GPC) for polymer molecular weight analysis was carried out with Waters system (515 HPLC pump, 2410 refractive index detector), Acme 9000 UV/Vis detector, and Shodex GPC LF-804 column eluted $CHCl_3$ (HPLC grade, J. T. Baker®). Flow rate was 1.0 mL/min and temperature of column was maintained at 35°C. Samples in 0.5-1.0 mg/mL $CHCl_3$ were filtered by 0.2um PTFE (Whatman®) filter before injection.

1.2.2 Synthesis of monomers

Diethyl dipropargylmalonate (M1)

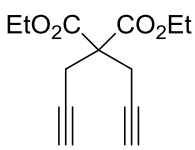

This monomer was prepared by the same method from the previous literature (Eglinton, G.; Galbraith, A. R. *J. Chem. Soc.* **1959**, 889.) ^{1}H, ^{13}C NMR and MS analysis data are also available in the same literature.

4,4−bis(acetyloxymethyl)−1,6−heptadiyne (M2)

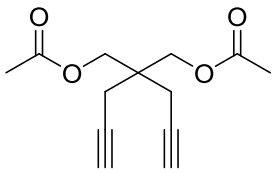

This monomer was prepared by the same method from the previous literature (Kim, S.−H.; Kim, Y.−H.; Cho, H.−N.; Kwon, S.−K.; Kim, H.−K.; Choi, S.−K. *Macromolecules* **1996**, *29*, 5422) ^{1}H, ^{13}C NMR and MS analysis data are also available in the same literature.

4−(2−Ethylhexanoyloxy)−methyl−1,6−heptadiyne (M3)

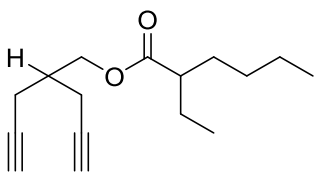

2−Ethylhexanoyl chloride (808.4 mg, 4.972 mmol) was added to the mixture of 4−hydroxymethyl−1,6−heptadiyne (**1**)[6] (432.6 mg, 3.541 mmol), triethylamine (1.075 g, 10.62 mmol), and DMAP (21.6 mg, 0.177 mmol) in dichloromethane (10 mL) at 0 °C. The mixture was stirred for 4 hr at room temperature then saturated $NaHCO_3$ aqueous solution was added. The mixture was washed with NH_4Cl aqueous solution and extracted by ethyl acetate (75 mL*3). The organic layer was dried with $MgSO_4$ and concentrated. Product was purified by column chromatography on silica gel (ethyl acetate:hexane = 1:30) to afford compound **M3** as a colorless liquid (830.9 mg, 94.5%). ^{1}H NMR (500 MHz, $CDCl_3$): δ 0.89 (t, J = 7.1 Hz, 3 H), 0.89 (t, J = 7.5 Hz, 3 H), 1.21−1.35 (m, 4 H), 1.43−1.67 (m, 4 H), 2.01 (t, J = 2.7 Hz, 2 H), 2.15 (hept, J = 6.4 Hz, 1 H),

2.28 (m, 1 H), 2.39 (dd, J = 2.7, 6.5 Hz, 4 H), 4.16 (d, J = 5.2 Hz, 2 H); ^{13}C NMR (125MHz, $CDCl_3$): δ 12.2, 14.3, 20.2, 23.0, 25.8, 30.0, 32.1, 36.7, 47.7, 65.1, 70.7, 81.2, 176.5; HRMS (EI+): calcd. for $C_{16}H_{24}O_2$, 248.1776, found, 248.1781.

4,4-Bis(benzyloxymethyl)-1,6-heptadiyne (M4)

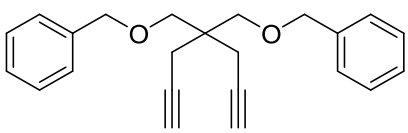

This monomer was prepared by the same method from the previous literature (Madine, J. W.; Wang, X.; Widenhoefer, R. A. *Org. Lett.* 2001, *3*, 385.) ^{1}H, ^{13}C NMR and MS analysis data are also available in the same literature.

4,4-Bis(octyloxymethyl)-1,6-heptadiyne (M5)

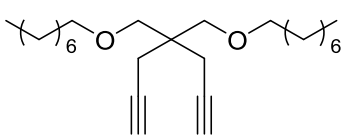

This monomer was prepared by the same method from the previous literature (Sudheendran, M.; Horecha, M.; Kiriy, A.; Gevorgyan, S. A.; Krebs, F. C.; Buchmeiser, M. R. *Polym. Chem.* 2013, *4*, 1590) ^{1}H, ^{13}C NMR and MS analysis data are also available in the same literature.

1.2.3 Preparation of catalyst

Second generation Grubbs catalyst (51.8 mg, 0.0610mmol) and 3-chloropyridine (1mL) were mixed in 20-ml sized vial for 5 minutes. Cold n-pentane was poured to the vial. After storage in freezer a few hours, the third generation Grubbs catalyst was

filtered and washed by pentane. The green product (39.1mg, 0.0491 mmol, 80.5%) was vacuum dried and stored in desiccator.

1.2.4 General polymerization procedure

Polymerization in DCM+additives system

Monomer was weighed in a 4-ml sized screw-cap vial with septum and purged with argon. DCM from solvent purification system was added to vial. The vial was placed in a cooler (at 0°C or 10°C). The solution mixture of initiator and additives (3,5-dichloropyridine 20mol% for monomer) was added at once under vigorous stirring. After confirming the monomer conversion by TLC, the reaction was quenched by excess ethyl vinyl ether. The polymer was purified by precipitation in methanol. The obtained solid was dried *in vacuo.*

Block copolymerization (Poly(M3)-b-poly(M2))

M3 was weighed in a 4-ml sized screw-cap vial with septum and purged with argon. DCM from solvent purification system was added to vial. The vial was placed in a cooler (at 0°C). The solution mixture of initiator and additives (3,5-dichloropyridine 20mol% for monomer) was added at once under vigorous stirring. After confirming the monomer conversion by TLC, solution of 2^{nd} monomer, M2, and additives was added at 0°C and reaction temperature was slowly increased to 10°C. After 3 hours, reaction mixture was quenched by excess amount of ethyl vinyl ether and purified by precipitation in methanol. The obtained solid was dried *in vacuo*

1.3 Result and Discussion

1.3.1 Screening additives & proper reaction conditions

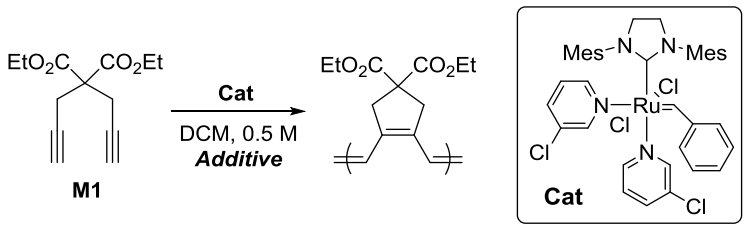

Entry	Additive	M/I/Add	Temp	Time	M_n[a] (g/mol)	PDI[a]	Conv[b] (%)
1	–	50/1/–	RT	1 h	12.6 k	2.56	68
2	–	50/1/–	0 °C	1 h	21.5 k	2.38	90
3	THF	50/1/20	RT	1 h	10.5 k	2.00	91
4	2,6−Cl_2BQ	50/1/10	RT	1 h	19.4 k	2.41	89
5	3,5−Cl_2Py	50/1/10	RT	1 h	26.4 k	1.13	>99
6	3,5−Cl_2Py	100/1/20	RT	1 h	39.7 k	1.62	90
7	3,5−Cl_2Py	100/1/20	10 °C	3 h	49.9 k	1.16	91

[a] Determined by $CHCl_3$ SEC calibrated using polystyrene (PS) standards. [b] Calculated from 1H NMR.

Table 1−1. Additive screening for polymerization of DEDPM (M1)

M1 was polymerized without any additive, resulting in 68% conversion at room temperature (Table 1−1, entry 1). On the other hand, monomer conversion at room temperature increased to 90% upon adding 40 mol% THF (Table 1, entry 3). Because it was difficult to handle very small amounts of liquid THF, we screened solid reagents as alternative additives. The first candidate was benzoquinone because it is known to inhibit the decomposition of Grubbs catalyst.[29] Adding 20 mol% of 2,6−dichlorobenzoquinone (2,6−Cl_2BQ) increased the conversion to 89% (Table 1−1, entry 4). However, in all the preceding cases, the PDIs of the resulting polymers were still very broad (> 2), leading us to speculate that the high catalyst activity resulted in an extensive chain transfer.

Assuming that the weakly coordinating ketone functionality of 2,6-Cl_2BQ might be responsible for the observed improvement in polymerization, we tested another solid reagent, 3,5-dichloropyridine (3,5-Cl_2Py), as a substitute for liquid 3-chloropyridine, a labile ligand already bound to Cat. Adding 20 mol% of 3,5-Cl_2Py led to the full conversion of M1 to polymer in 1 h at room temperature, with a surprisingly narrow PDI of 1.13 (Table 1-1, entry 5). Increasing M/I to 100 led to high conversion of M1 at room temperature, along with significantly broadening the PDI.

Interestingly, we found that lowering the reaction temperature could increase the monomer conversion (Table 1-1: entry 1 vs. 2) and also suppress the chain transfer resulting successfully reduced the PDI from 1.62 to 1.16 (Table 1-1, entries 6 and 7). It demonstrates that not only conversion with the DCM solvent system can be improved but also controlled polymerization can be achieved by adding appropriate additive(s).

1.3.2 Molecular weight of polymers

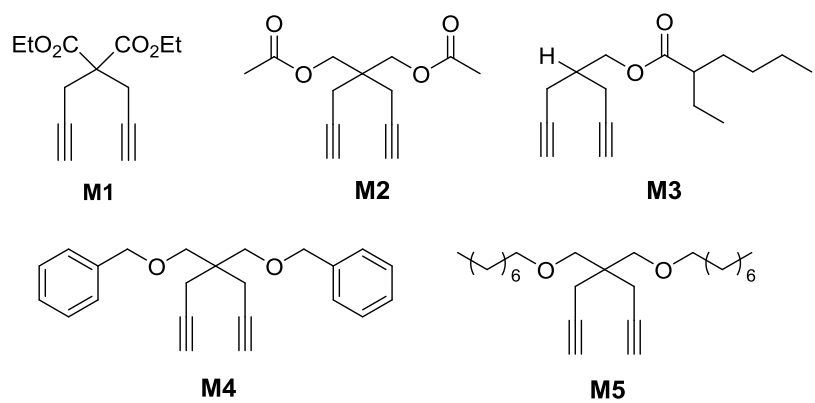

Figure 1-1. Various monomers used for controlled polymerization.

M1 and several other 1,6-heptadiyne derivatives were tested for controlled CP under the optimized reaction conditions (20 mol% of 3,5-Cl_2Py) (Figure 1-1). Various monomers (M1 – M4) were successfully polymerized in a controlled manner to afford

polymers with molecular weights directly proportional to the M/I ratio and with narrow PDIs in the range 1.08–1.31 (Table 1-2 and Figure 1-2).

Table 1-2. Polymerization of various monomers

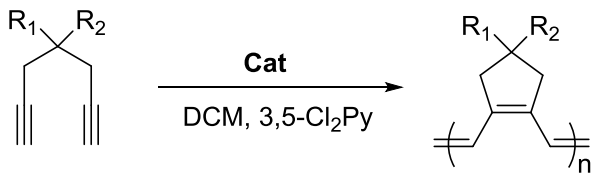

Entry	M	M/I/Add	Temp (°C)	Time (h)	M_n[a] (g/mol)	PDI[a]	Conv[b] (%)
1	**M1**	25/1/5	10	3 h	12.4 k	1.13	>99
2	**M1**	50/1/10	10	3 h	23.4 k	1.13	97
3	**M1**	75/1/15	10	3 h	36.5 k	1.15	93
4	**M1**	100/1/20	10	3 h	49.9 k	1.16	91
5	**M2**	25/1/5	10	3 h	12.0 k	1.10	>99
6	**M2**	50/1/10	10	3 h	22.7 k	1.12	97
7	**M2**	75/1/15	10	3 h	30.2 k	1.12	97
8	**M2**	100/1/20	10	3 h	40.7 k	1.15	95
9	**M2**	150/1/30	10	3 h	53.3 k	1.18	91
10	**M3**	25/1/5	0	0.5 h	8.4 k	1.13	>99
11	**M3**	50/1/10	0	1 h	18.6 k	1.09	>99
12	**M3**	75/1/15	0	1.3 h	31.3 k	1.12	>99
13	**M3**	100/1/20	0	3 h	39.8 k	1.13	>99
14	**M3**	150/1/30	0	3 h	67.7 k	1.17	>99
15	**M3**	200/1/40	0	3 h	72.4 k	1.31	>99
16	**M4**	25/1/5	10	1.5 h	10.0 k	1.11	>99
17	**M4**	50/1/10	10	2 h	27.1 k	1.08	>99
18	**M4**	75/1/15	10	2.5 h	34.7k	1.14	>99
19	**M4**	100/1/20	10	3 h	42.2 k	1.18	97
20	**M5**	50/1/10	10	3 h	28.3 k	1.26	>99

[a] Determined by CHCl3 SEC calibrated using polystyrene (PS) standards. [b] Calculated from 1H NMR.

Figure 1-2. Plots of M_n vs. M/I and corresponding PDI values for poly(M1) through poly(M4). The actual M/I values were calculated from the initial feeding ratios and the final monomer conversions

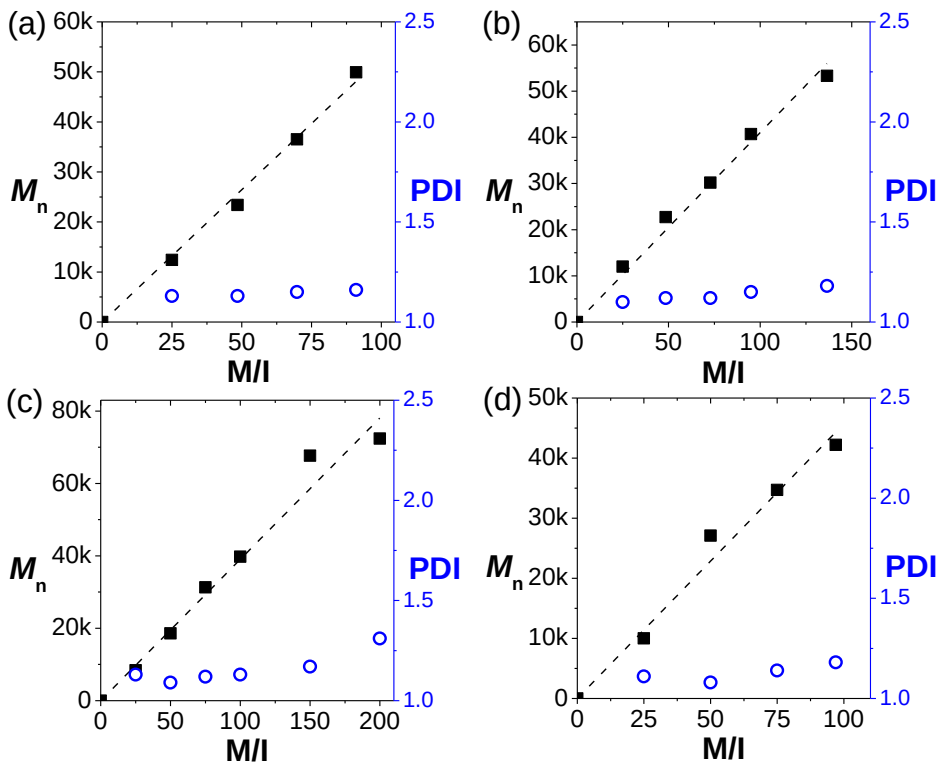

In our previous work in THF,[24-25] we could only use monomers containing longer alkyl groups or bulky moieties that could overcome the solubility problems typical of conjugated polyenes. Now, with the improved solubility of DCM, monomers containing short side chains (M1 and M2) could yield polymers with high Mn values (up to 50 k) and narrow PDIs (Table 1-2, entries 1-9; Figures 1-2a and 2b). Polymerization of mono-substituted ester M3 in THF (M/I = 100) resulted in a broad PDI (2.23), even at −10 ℃, because a relatively small side-chain could not effectively suppress the chain transfer. In contrast, with 20 mol% of the pyridine additive, CP of M3 in DCM at 0 ℃ produced polymers with a high degree of polymerization (DP) of 200 and narrow PDIs (Figure 1-2c and Table 1-2, entries 10–15). This demonstrated

that the new DCM reaction conditions with the right additive could provide better control than the THF conditions. Controlled polymerization was also possible with ether-containing M4, demonstrating an even greater monomer scope (Figure 1-2d and Table 1-2, entries 16–19). Meanwhile, M5, which had previously been polymerzed using Schrock catalysts to yield polymers with a broad PDI (2.4),[30] yielded polymers with a much narrower PDI (1.26) using the new DCM system (Table 1-2, entry 20). In brief, the use of coordinating additives in DCM has significantly expanded the monomer scope of controlled CP.

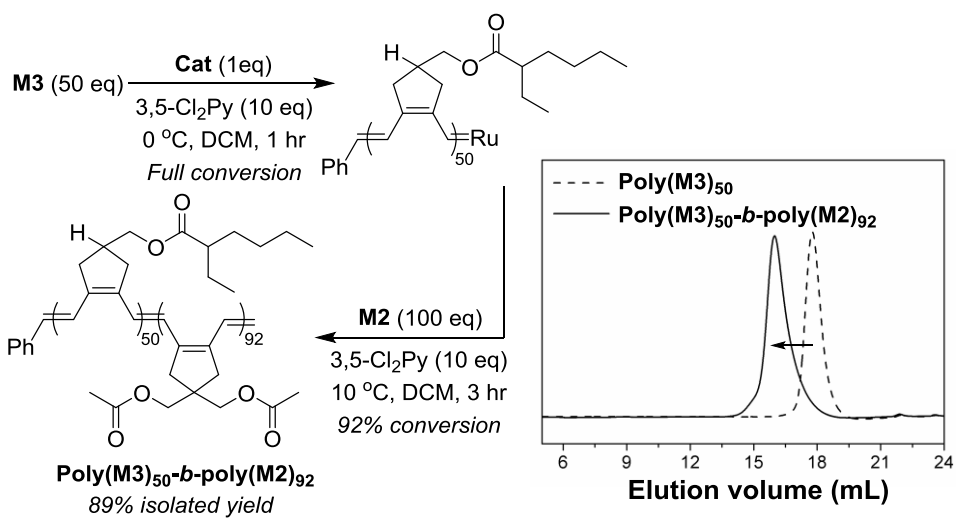

Figure 1-3. Block copolymerization of M3 and M2 in DCM and SEC traces for poly(M3)$_{50}$ (M_n = 17.5 k, PDI = 1.11) and poly(M3)$_{50}$-*b*-poly(M2)$_{92}$ (M_n = 56.2 k, PDI = 1.29).

To show that living CP is possible in DCM, block copolymerization was attempted. Fully conjugated diblock copolymer was successfully prepared from 50 equivalents of M3 (with respect to catalyst loading) in DCM at 0 ℃ following with the addition of 100 equivalents of M2 at 10 ℃ to produce poly(M3)-b-poly(M2) in 89% isolated yield (Figure 1-3a). Block copolymerization was confirmed using SEC, which revealed an increase in Mn from 17.5 k to 56.2 k upon adding a second monomer; narrow PDIs (<1.3) were

successfully maintained throughout the process (Figure 1-3b). These conditions were more efficient than those of our previous work, because they allowed the doubling of the degree of polymerization for each block.[24]

To understand how additives improve the CP, we designed 1H NMR experiments to observe how additives affect the propagating carbene and overall conversion. We began by determining the chemical shift of the propagating carbene, mixing a 10:1 ratio of M1 and Cat in deuterated DCM (DCM-d_2) and obtaining the 1H NMR spectra after full conversion (Figure 1-4a, (i) and (ii)). The initial benzylidene moiety in Cat was observed at 19.1 ppm; upon adding M1, new propagating carbenes began to appear at 19.8 ppm. Similarly, with the pyridine additive, the chemical shift for the carbene changed from 19.1 ppm to 19.7 ppm upon the addition of M1 (Figure 1-4a, (iv)). Based on these assignments, it becomes possible to monitor changes in the total propagating carbene signals over time by plotting time vs. percentage of the remaining propagating carbene (carbene%).

Initially, we monitored the carbene signals for the CP of M1 with M/I = 10 at room temperature without additives; as shown in Figure 1-4b, carbene% drastically declined early in the reaction before leveling out at less than 50% of the initial carbene concentration (black line). However, we observed much higher carbene% of up to 80% remaining for an otherwise identical reaction with 3,5-Cl_2Py added (red line). Moreover, almost no change in carbene% occurred during reaction in deuterated THF (THF-d_8) (blue line). At this point, it is unclear how the propagating carbene decomposes, but it does appear as though weakly coordinating species such as pyridine additives or THF suppress or retard this process.

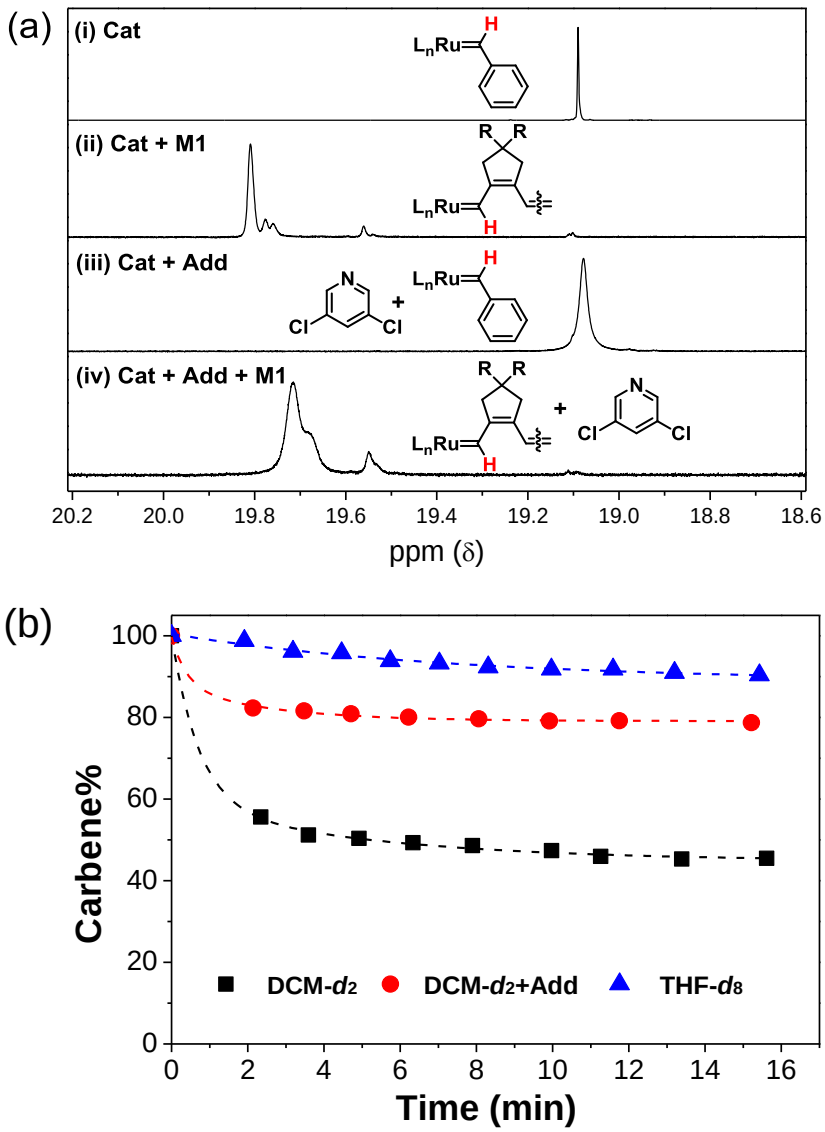

Figure 4. (a) ^{1}H NMR spectra of the initial and propagating carbene of **Cat** and **Cat** + additive in DCM−d_2. (b) Decrease in the carbene signal over time during CP (M/I = 10). Remaining carbene% was calculated from ^{1}H NMR using hexamethyl disilane as an internal standard.

1.4 Conclusion

In summary, we demonstrated successful CP of 1,6-heptadiyne derivatives in DCM using the third-generation Grubbs catalyst and 3,5-Cl2Py. Various monomers were successfully polymerized through living polymerization to afford polymers with excellent molecular weight control and narrow PDIs. Mechanistic studies using 1H NMR revealed that weakly coordinating reagents (THF and 3,5-Cl_2Py) suppressed the decomposition of the propagating carbene (a 14-electron state) and increased the turnover numbers of the reactions. Kinetic analyses of the reaction order showed that living polymerization was possible in the presence of weakly coordinating reagents at lower temperatures, because the propagating carbenes were stabilized and chain transfer was suppressed. Consequently, block copolymer with molecular weight higher than those shown in the previous report was successfully produced. In brief, an improved understanding of the mechanistic details of CP in DCM allowed for the targeted modification of the reaction conditions, significantly enhancing the monomer scope and utility of the reaction.

Part 2 :
Solvent aging experiment of *In-situ* Nanoparticlization of conjugated polymers

2.1 Introduction

Meldrum's acid derivatives have gotten big attention in organic chemistry for their potential to use as precursors to highly electrophilic ketenes since the first synthesis by Meldrum in 1908.[31] Recently, Hawker reported the mild preparation of ketenes from polymers containing Meldrum's acid, and these ketene were used to cross-link the polymer or introduce various functional groups to the polymer chain.[32, 33]

Previously, our group applied Meldrum's acid moiety to the synthesis of conjugated polymers by cyclopolymerization using a third-generation Grubbs catalyst. However, we cannot characterize the *poly(1)* by itself because of its insolubility. Therefore we synthesized block copolymer with soluble monomers for further analysis. Interestingly, we observed *in-situ* self-assembly behavior of the diblock copolymers.[34] Furthermore, we observed conformational changes from initially generated nanostructures by solvent aging process; Spherical micelle to worm-like micelle via irradiating light to the polymer solution was observed in case of block copolymer **A**.

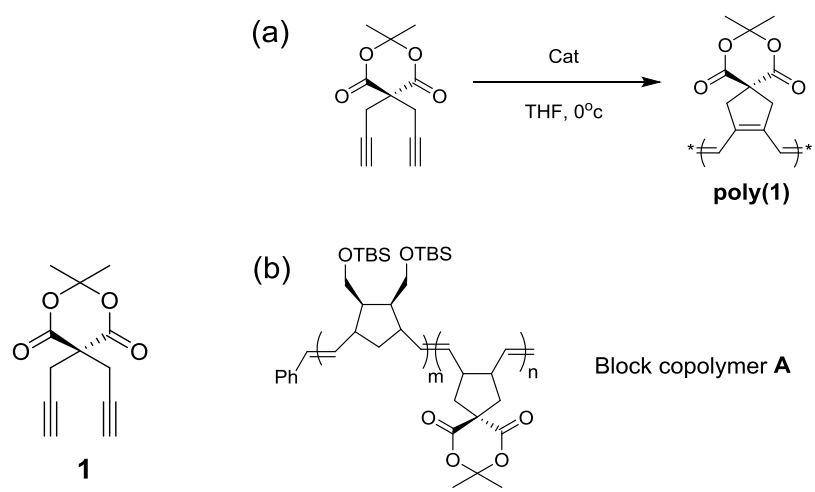

Figure 2-1. 1,6-heptadiyne moiety containing Meldrum's acid (1)

and (a)Synthetic scheme of the conjugated polymer using 1 (b)Chemical structure of block copolymer A used in previous experiment.

These self-assemblies of block copolymer nanoparticles were possible without any additional reagents except light. From previous works, we analyzed the conformational changes from single spherical micelles (0D) to cylindrical micelles (1D) and even network structures (2D) using block copolymer A.

In this study, we studied further conformational changes induced by solvent aging process using diblock copolymer which containing Meldrum's acid moiety as core. To induce bigger formation of association, we thought more solvophobic core have to be exposure. So we changed 1st block from norbornene moiety to TD moiety which had lower solubilizing ability than NB moiety due to rigidity.

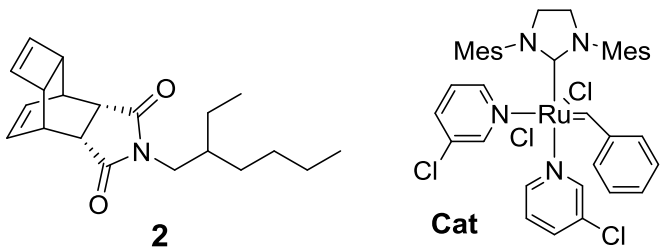

Figure 2-2. Chemical structure of 2 and Grubbs catalyst for the polymerization

Indeed, the reacitivity ratio between norbornene (NB) and endo-tricyclo[4.2.2.0]deca-3,9-diene (TD) was large to make gradient copolymer; reactivity to the catalyst of TD is faster than NB due to fast initiation rate.[35] In addition to, we even got the larger reactivity ratio to the catalyst for NB moiety than MA substituted 1,6-heptadiyne previously.[34] Therefore, we tried *in-situ* nano-particlization of gradient copolymers synthesized via *one-shot* polymerization method which is simple and easy.

Monomer **2** used as solubilizing block with **1** and was polymerized using third-generation Grubbs catalyst. As we expected, gradient copolymer was synthesized by one-shot method, and it showed larger aggregates by solvent aging process. Detailed analysis was done using Dynamic light scattering (DLS), Atomic Force Microscopy (AFM), Transmission Electron Microscopy (TEM), UV-Vis spectroscopy and so on.

2.2 Experimental

2.2.1 General experimental

All reactions were carried out under dry argon atmosphere using standard Schlenk-line techniques. Solvents for monomer synthesis were commercially obtained. For polymerization, tetrahydrofuran (THF) was distilled from sodium and benzophenone. THF was degassed for 10 minutes before using on polymerization. 1H NMR and 13C NMR were recorded by Varian/Oxford As-500 (500 MHz for 1H and 125 MHz for 13C) spectrometer and Agilent 400-MR (400 MHz for 1H and 100 MHz for 13C). Gel permeation chromatography(GPC) for polymer molecular weight analysis was carried out with Waters system (515 HPLC pump, 2410 refractive index detector), Acme 9000 UV/Vis detector, and Shodex GPC LF-804 column eluted $CHCl_3$ (HPLC grade, J. T. Baker®). Flow rate was 1.0 mL/min and temperature of column was maintained at 35°C. Samples in 0.5-1.0 mg/mL $CHCl_3$ were filtered by 0.2um PTFE (Whatman®) filter before injection. Multimode 8 and Nanoscope V controller (Vesco Instrument) were used for AFM imaging. Dynamic Light Scattering (DLS) data were obtained by Malvern Zetasizer Nano ZS.

2.2.2 Synthesis of monomers

2,2-dimethyl-5,5-di(prop-2-ynyl)-1,3-dioxane-4,6-dione (1)

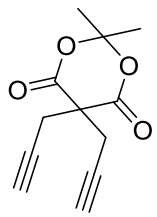

This monomer was prepared by the same method from the previous literature (Kim. J.-E.; Kang. E.-H.; Choi. T.-L. *ACS Macro Lett.* 2012, *1*, 1090-1093.) ^{1}H, ^{13}C NMR and MS analysis data are also available in the same literature.

Anhydride endo-tricyclo[4.2.2.0^{2,5}]deca-3,9-diene (2)

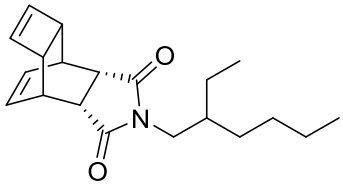

This monomer was prepared by slightly modified method from the previous literature. (Kim, K. O.; Choi, T.-L. *Macromolecules* 2013, *46*, 5905.) White solid. 1H NMR (500 MHz, $CDCl_3$): δ 2.81 (s, 2 H), 3.07 (s, 2 H), 3.24 (s, 2 H), 5.91 (s, 2 H), 6.04 (t, 2 H); 13C NMR (125 MHz, $CDCl_3$): δ 36.83, 43.24, 43.88, 129.04, 138.16, 172.68. HRMS (EI+): 313.2042 (calc.), 313.2038 (found).

2.2.3 Preparation of catalyst

Second generation Grubbs catalyst (51.8 mg, 0.0610mmol) and 3-chloropyridine (1mL) were mixed in 20-ml sized vial for 5 minutes. Cold n-pentane was poured to the vial. After storage in freezer a few hours, the third generation Grubbs catalyst was filtered and washed by pentane. The green product (39.1mg, 0.0491 mmol, 80.5%) was vacuum dried and stored in desiccator.

2.2.4 General polymerization procedure

Block copolymerization

2 was weighed in a 4-ml sized screw-cap vial with septum and purged with argon. Distilled THF was added to vial. The solution mixture of initiator was added at once under vigorous stirring at room temperature. After confirming the monomer conversion by TLC, solution of 2nd monomer, **1** was added. Reaction was quenched by excess amount of ethyl vinyl ether and purified by precipitation in methanol. The obtained solid was dried *in vacuo*

One-shot copolymerization

Monomer **1** and **2** was weighed in a 4-ml sized screw-cap vial with septum and purged with argon. Distilled THF was added to vial. The solution mixture of initiator was added at once under vigorous stirring at room temperature. After 2 hours, the reaction was quenched by excess amount of ethyl vinyl ether and purified by precipitation in methanol. The obtained solid was dried *in vacuo*

2.2.5 Atomic Force Microscopy (AFM)

The atomic force microscopy experiments were performed with a thin film prepared by spin-coating of one drop of the polymer solution (~0.01mg/ml. $CHCl_3$, spinning rate = 3000rpm for 30 sec.) The polymer solution The thin films were prepared on mica. Images were obtained on tapping mode using non-contact mode tips from Nanoworld (Pointprobe® tip, NCHR type) with spring constant of 42 Nm^{-1} and tip radius of $\leq$8nm.

2.2.6 Transmission Electron Microscopy (TEM)

The samples for TEM were prepared by drop-casting 10 μL aliquot of the polymer solution (0.005 mg polymer/mL $CHCl_3$) onto a carbon coated copper grid which was placed on a piece of paper to get rid of excess solvent. This polymer thin film was dried *in vacuo* for 3h. The images were obtained on JEM-2100 (JEOL) in the National Center for Inter-University Research Facility (NCIRF) at SNU

2.3 Results and discussion

2.3.1 One-shot polymerization method

Firstly, we monitored monomer conversion using ^{1}H NMR to confirm our assumption; gradient copolymer using **1** and **2** as monomer through the *one-shot* polymerization.

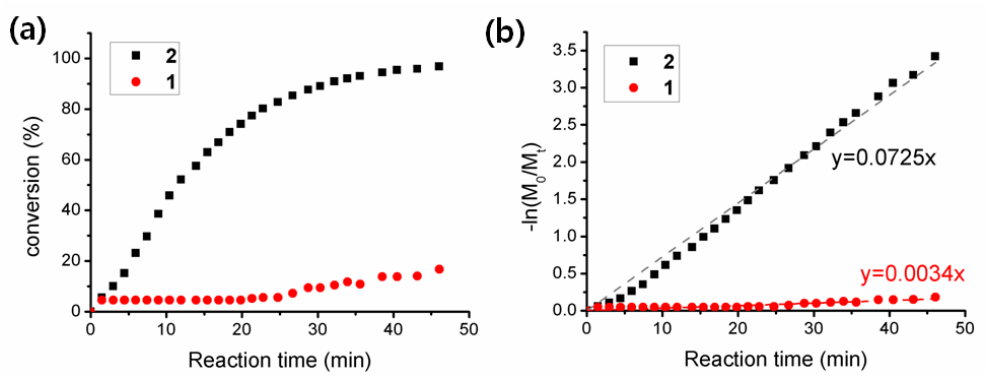

Figure 2-3. (a) Plots of conversion(%) vs. time for monomer **1** and **2** (b) Plots of $-\ln([M_0]/[M_t])$ vs. time for monomer **1** and **2**

The monomer conversion of **1** and **2** showed big differences.

(Figure 2-3a) Until about 30 minutes, the conversion of **2** reached 90% whereas the conversion of **1** was less than 10%. The conversion of **1** started to increase after almost all **2** was consumed. To figure out the difference of rate constants for each monomer, we plotted logarithmic conversion vs. time. (Figure 2-3b) It showed that the rate constant for **2** is about 20 times larger than **1**, and this difference was enough to make gradient copolymer rather than random copolymer.

Then, we fixed the feeding ratio as **1** : **2** = 50 : 30 considering the reaction time and possibility to induce larger conformational changes after screening.

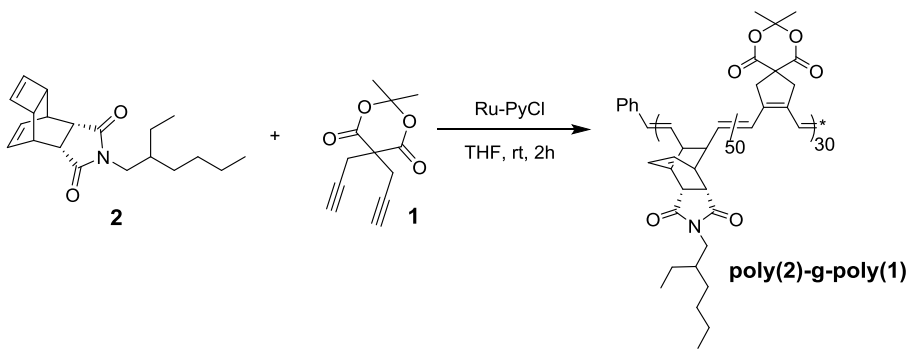

Scheme 2-1. *One-shot* polymerization using 1 and 2 as monomer

2.3.2 *In-situ* Nanoparticlization using gradient copolymer

By using *one-shot* polymerization method, we could get the core-shell nanostructures. This was firstly confirmed by ^{1}H NMR analysis of copolymer. (Figure 2-4) There were no signals corresponding to poly(**1**) and signals corresponding to the homopolymers of **2** even though the cyclopolymerization of **1** occurred with full conversion. It indicated that polymerization induced self-assembly occurred during the polymerization to afford nanoparticles consisting of the insoluble poly(**1**) as the core and the soluble poly(**2**) as the shell.

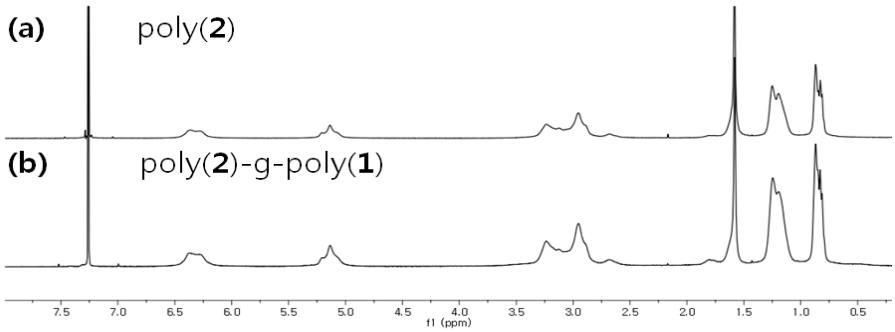

Figure 2-4. ^{1}H NMR of (a) poly(**2**) (b) poly(**2**)-*g*-poly(**1**)

SEC trace also supported formation of self-assembly by showing two sets of traces. (Figure 2-5a) Trace with much higher molecular weights ($M_{n,m}$ in Table 2-1) than expected for the single chain seemed to be related to the nanoparticles containing the poly(**1**) as core. The other trace which came out around 18min seemed like corresponding to the single chain of copolymers. ($M_{n,s}$ in Table 2-1) The λ_{max} of this nanoparticle was 481nm (Figure 2-5b)

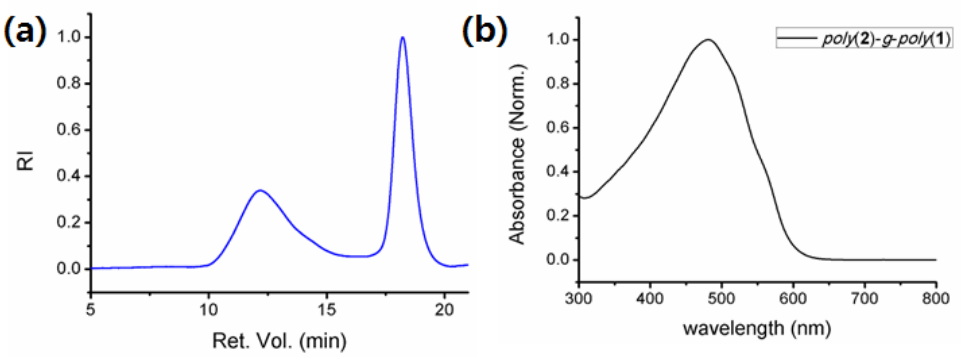

Figure 2-5. (a) SEC trace (b) UV spectra of *poly(2)-g-poly(1)*

Entry	1:2:cat	$M_{n,m}$	PDI_m [a]	$M_{n,s}$	PDI_s [b]
1	50:30:1	429 k	2.28	14.7 k	1.12

[a] Values corresponding to the micelle. [b] Values corresponding to the polymer single chain determined by SEC eluted by $CHCl_3$ and calibrated using polystyrene (PS) standards.

Table 2-1. Gradient copolymer of poly(**2**) with poly(**1**)

To investigate the self-assembly in detail, structural information of these nanoparticles was obtained using dynamic light scattering (DLS) analysis, atomic force microscopy (AFM) and transmittance electron microscopy (TEM)

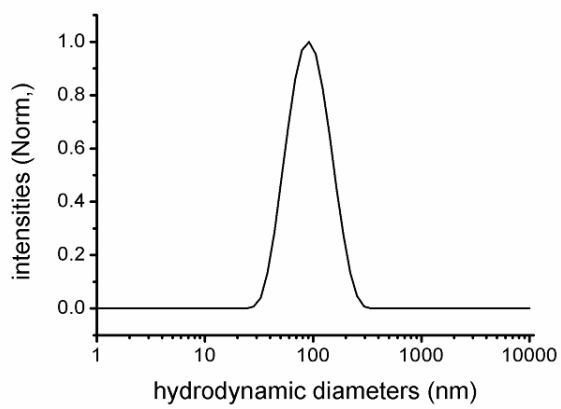

Figure 2-6. Hydrodynamic radius diagram from the solution of poly(**2**)-g-poly(**1**) in $CHCl_3$ (1mg/ml) obtained by dynamic light scattering. Average hydrodynamic diameter is 111.9nm.

From DLS analysis, we got the size information of nanostructure had an average diameter of 112 nm in chloroform solution. For AFM imaging, dilute solution of polymer in chloroform was spin-coated onto mica and via tapping mode, and the mixture of spherical and worm-like micelles with average height 5.50 (± 1.30) were observed (Figure 2-7a). In addition, TEM image also gotten for same solution prepared by drop-casted onto carbon coated copper grid. It showed well matched results with AFM and DLS.

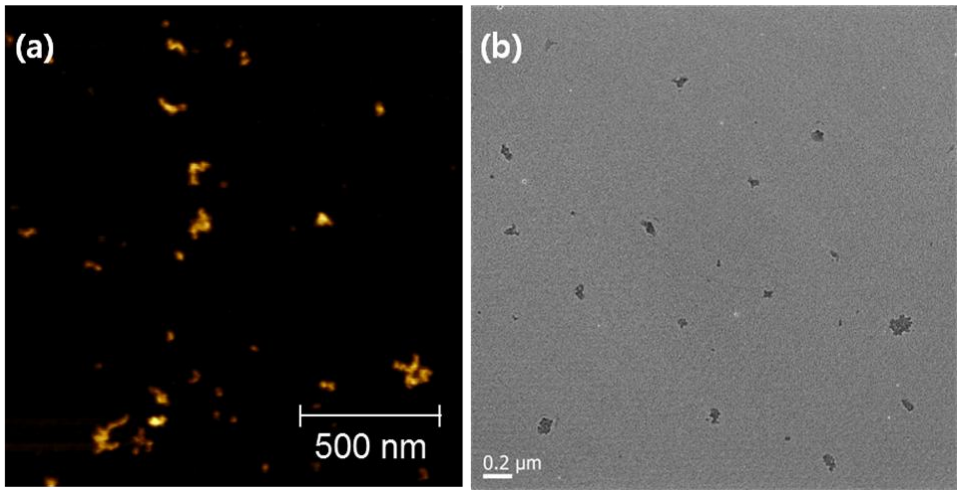

Figure 2-7. (a) AFM (b) TEM image of poly(2)-g-poly(1)

2.3.3 Solvent Aging process

In our previous work using NB moiety as shell and Meldrum's acid substituted PA derivative as core, we observed spontaneous nanocaterpillar formation from spherical core-shell structure by solvent aging. We assumed the driving force to induce these conformational changes was *cis* to *trans* isomerziation of conjugated polymers because we observed red-shifted spectra and increased intensity of the 0-0 vibronic peak in the absorption spectra corresponds to a more extended conformation for CPs.[36] In previous work from our group, coil to rod transition of conjugated polymers (CPs) was observed and this transition was induced by isomerization of *cis* component of conjugated polymer via radical mechanism.[37] In addition to, These isomerization was accelerated by irradiating blue LED.

Considering isomerization of CPs as critical factor to induce conformational changes, we used chloroform (without radical stabilizer) and blue LED light to induce isomerization much quickly.

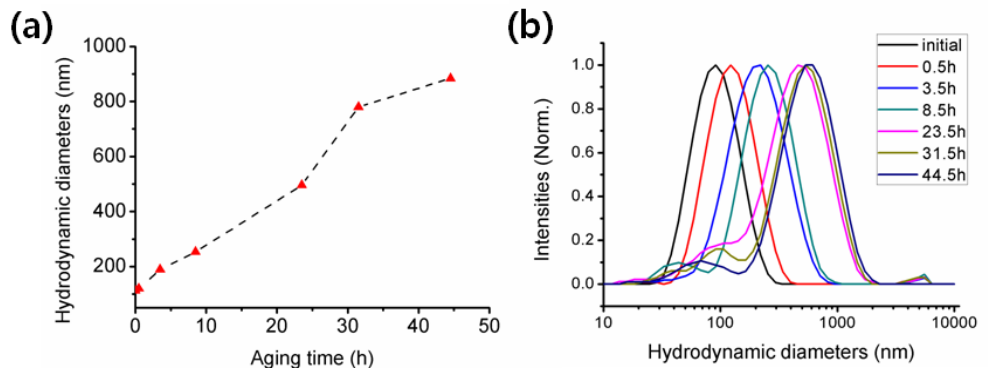

Figure 2-8. (a) Tendency of increment of Average hydrodynamic diameters (b) changes in hydrodynamic diameters in terms of solvent aging time. (Aging condition: 1mg/ml chloroform solution)

As aging time went by, the hydrodynamic diameters were gradually increased up to 884nm, and the average hydrodynamic volume started to decrease after about 45 hours. (Figure 2-8a, Table 2-2) Traces of DLS were clearly shifted to right corresponding to aging time until 44.5 hours. (Figure 2-8b)

Aging time (h)	λ max (nm)	Diameter (nm)	S factor
0	481	111.9	-
0.5	497	119.9	1.60
3.5	527	188.7	1.38
8.5	527	253.5	1.36
23.5	527	495.4	1.36
31.5	526	779.9	1.36
44.5	526	884.1	1.37
59.5	525	799	1.40
85	524	708.3	1.42
100	492	670.6	1.62
171	broken	87.22	-

Table 2-2. λ max, hydrodynamic diameters, Huang-Rhys factor, S factor, in terms of solvent aging time for poly(**2**)-g-poly(**1**)

We also measured UV−Vis spectrum in terms of aging time and calculated Huang−Rhys factor. This Huang−Rhy factor, S factor, is a theoretical prediction of the configurational displacement of the potential energy curve upon electronic excitation.[38] (Table 2−2, Figure 2−9a)

Absorption spectra showed red−shifts corresponding to aging time and S factor was decreased to minimum value, 1.36, after 8.5 hours. It was hard to say that extension of core fully occurred after 8.5 hours because there were other factors from nanostructures. However, this observation indirectly suggested conformational changes to more extended and planar of core was occurred.

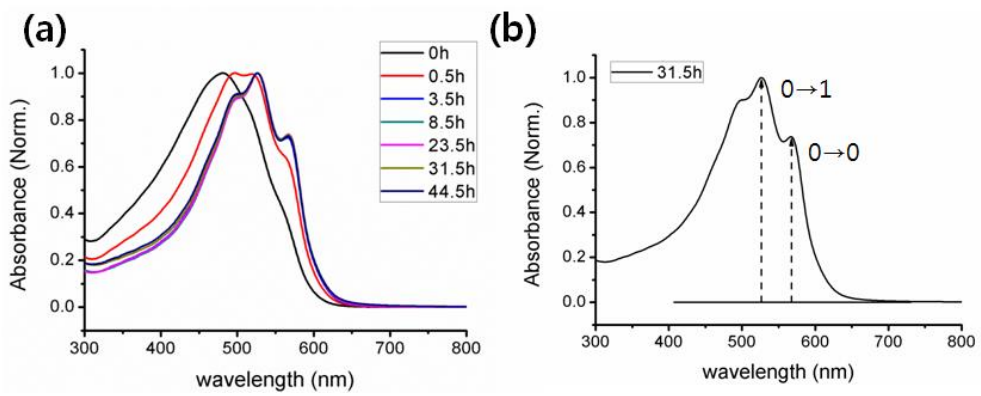

Figure 2−9. (a) UV−Vis spectrum corresponding to solvent aging times (b) $I_{1\leftarrow0}$, $I_{0\leftarrow0}$ for 31.5h aged sample; S= $I_{1\leftarrow0}/I_{0\leftarrow0}$

We did control experiment to see the isomerization effect. Firstly, we made polymer solution which had same condition except the light. We blocked the light by covering with aluminum foil and put it in the hood. From this control experiment, we observed that hydrodynamic diameters barely changed and changes absorption spectra was small comparing with irradiated one. (Figure 2−10a, b, c)

Secondly, the associating rate was also slowed down when aging solvent, chloroform, contained radical stabilizer. (100–200ppm Amylenes) (Figure 2–10d) Those observations also strongly supported that *cis* to *trans* isomerization was the driving force of interparticular association because isoemrization of CPs was fasten by Blue LED and occurred via radical pathway.

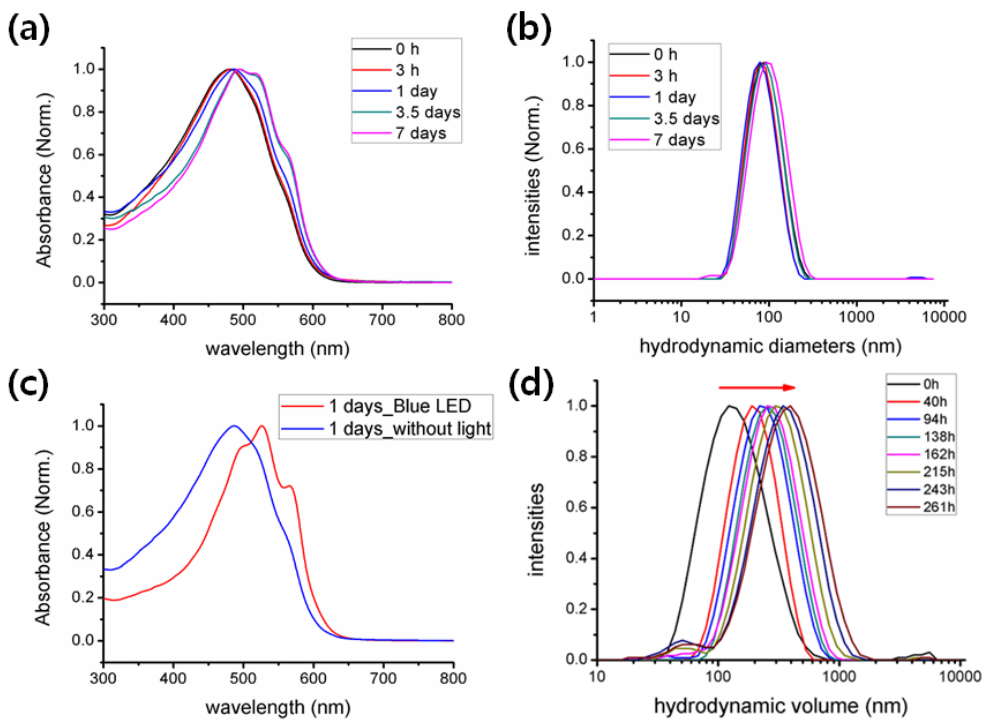

Figure 2–10. Changes of (a) UV–Vis spectra (b) hydrodynamic diameters in terms of aging time when light source was absent. (c) Different result of absorption spectra corresponding to light. (d) Changes of hydrodynamic diameters when radical stabilizer contained.

To figure out the detailed information of conformational changes, atomic force microscopy (AFM) and transmission electron microscopy (TEM) were used.

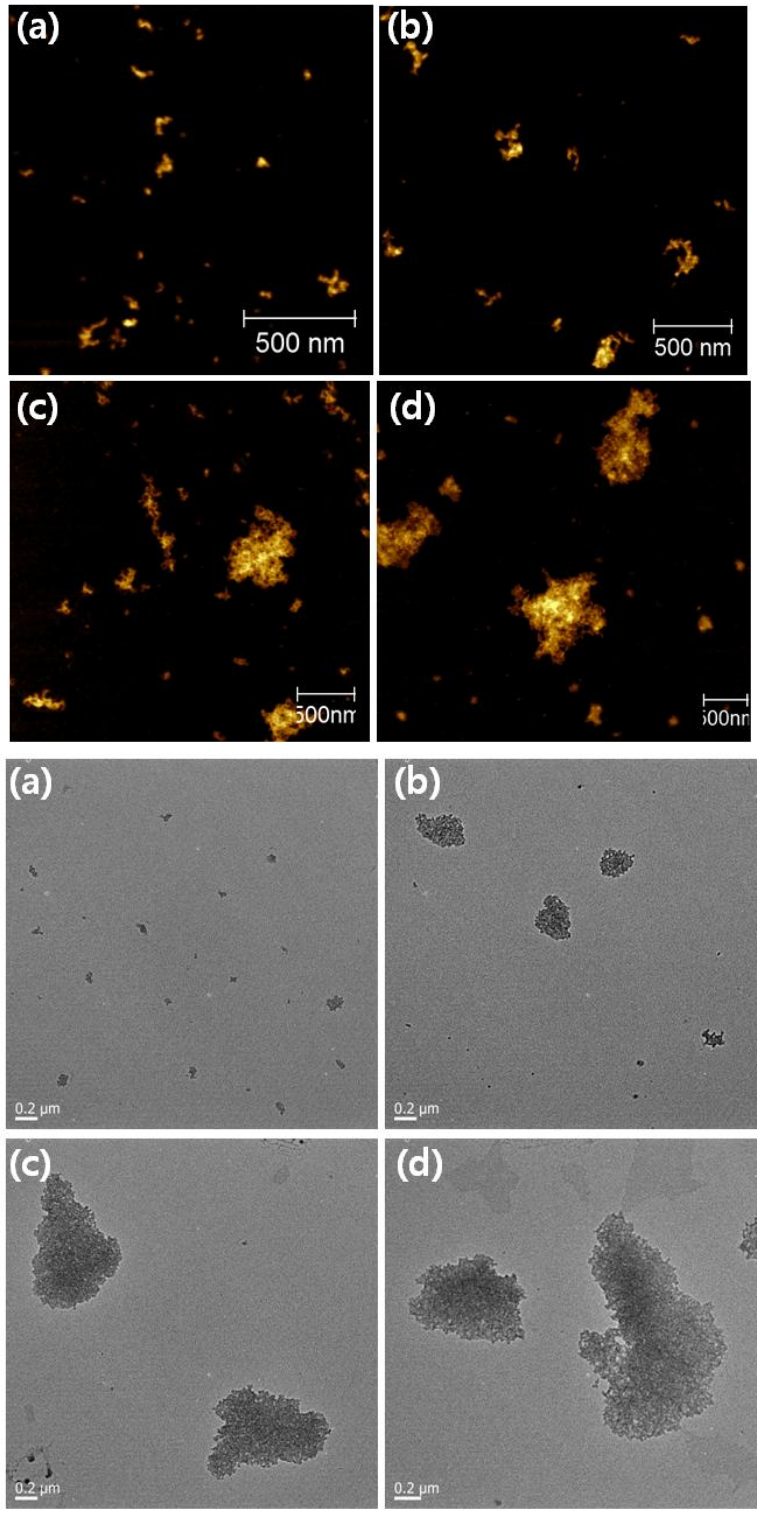

Figure 2-11. AFM and TEM images of (a)initial (b) 8.5 h (c) 23.5 h (d) 31.5h aged samples.

By the result of DLS, the distribution of nanostructures was quite large and even increased as aging time increased. (Figure 2-8b) Therefore, the sizes of aggregates were not regular in AFM and TEM images. However, these images showed clear effect of solvent aging process. After 8 hours, mixture of spherical and worm-like nanostructures was attached each other to make aggregated structures in AFM images, (Figure 2-11) and the height and size of aggregates increased in terms of aging time; height 5.50 (± 1.30)nm → 6.97 (± 1.68)nm → 8.44(± 2.40)nm → 11.70(± 2.85) nm.

This tendency was also confirmed by TEM by showing increased size of aggregated core according to the aging time. These images show the solvent aging effect visually and also well matched with the changes of hydrodynamic diameters measured by DLS.

2.3.4 Mechanical stability & Reversibility

After inducing conformational changes, we wanted to check the stability of final structures. Therefore, we checked the thermal and mechanical stability using heat and sonicator.

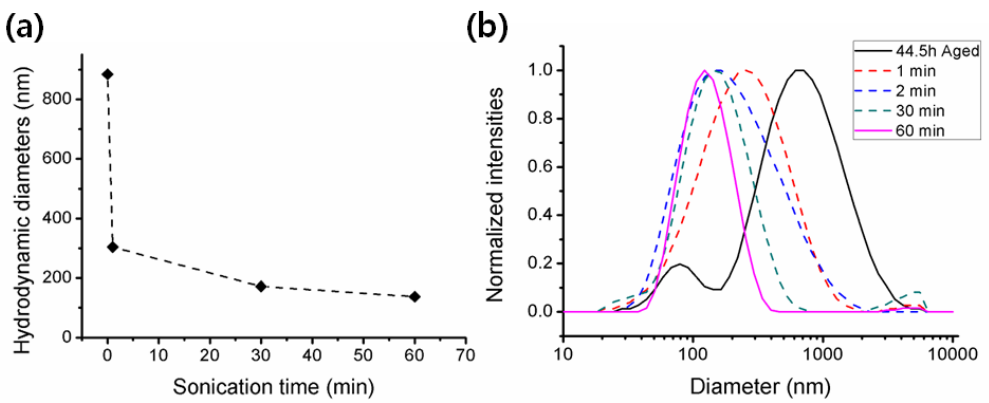

Figure 2-12. (a) Tendency of decrement of Average hydrodynamic diameters (b) changes in hydrodynamic diameters in terms of sonication times.

From DLS measurement, we observed gradual decreases occurred corresponding to sonication time. Even after 1 minute of sonication led prompt decrease of hydrodynamic diameters; 884 nm → 304 nm. It means mechanical stability of nanoparticles induced by solvent aging process was not high enough to maintain their structures contrary to high stability of initial structure of nanoparticles formed during polymer synthesis. However, hydrodynamic diameters in terms of sonication times were always larger than initial value regardless of sonication time. (Figure 2-12)

These phenomena were quite reasonable considering the solvophobic interaction as driving force of interparticular association. As mentioned, isomerization was critical factor for association. That is, the extension of core induced by isomerization caused the exposure of solvophobic core. After exposure of solvophobic core, associations finally occurred for minimal contact with solvent. So, interaction between nanoparticles was not strong to maintain their structure during sonication. Also, the reason of limited decreases via sonication seemed core extension of each nanoparticle itself which was initially formed.

If solvophobic interaction induced via isomerization was driving force of interparticle association, re-attachment after dissociation should be obtained because the exposure of solvophobic core still existed after sonication. Therefore, we checked the reversibility of association and dissociation behavior. For re-association, we did not irradiate light because we thought meaningful extension of core was already done.

Firstly, we confirmed whether re-association occurred. When we checked the hydrodynamic diameters after first sonication which dissociated from 880nm to 140nm, we could observe the gradual increases as time went by; 140nm → 490nm (after 17 hours) → 1,500 nm (after 45 hours). (Table 2-3)

Then we checked reversibility of this process. After getting re-associated one, we repeated the sonication and re-assocation process. Good reproducibility was gotten. (Figure 2-13, table 2-3)

Sample name	Sonication time (min)	Time for re-association (h)	Hydrodynamic diameters (nm)
S1	60		137.2
R1		45	1529
S2	60		186.3
R2		44	1364
S3	60		183.2
R3		44	1304

Table 2-3. Changes of average hydrodynamic diameters as repeating sonication and re-aging process

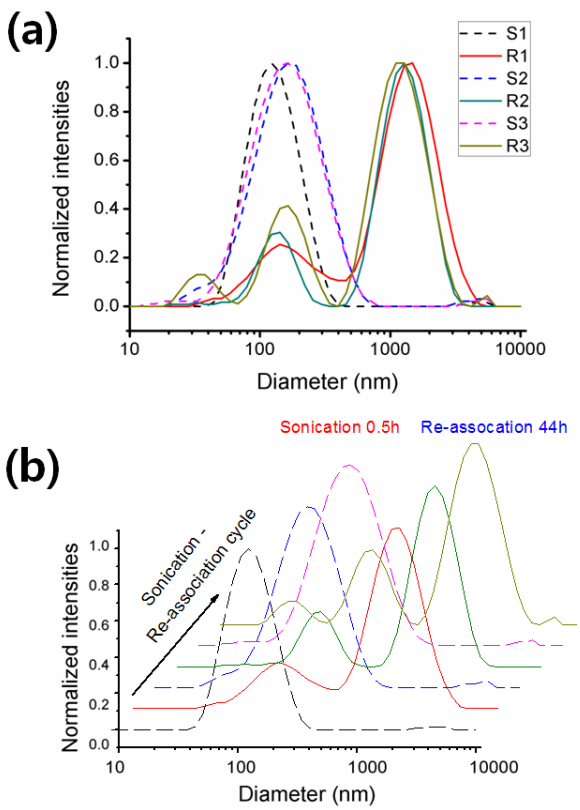

Figure 2-13. Hydrodynamic diameters for soncation - Re-association cycle

2.4 Conclusion

In summary, we demonstrated interparticular association of gradient copolymer, poly(**2**)-*g*-poly(**1**), via solvent-aging process. As aging time increased, associations of particles were occurred and induced big conformational changes. From AFM and TEM images, we could see the conformational changes visually. We thought the reason why those interparticular associations occurred was the solvophobic interactions between exposed cores which was induced by core extension. We guessed the core extension was occurred by *cis* to *trans* isomerization of conjugated backbone of core, and results from absorption spectra supported it indirectly through the increased intensity of vibronic peak which means changes to more extended and planar of CPs in terms of aging time. In addition to, those interparticular associations induced by aging process showed lower stability to mechanical force but re-association was possible. So it showed the possibility to make reversible conformational changes using nanoparticles which were prepared *in-situ*.

Reference

(1) Choi, S.-K.; Gal, Y.-S.; Jin, S.-H., Kim, H. K. *Chem. Rev.* 2000, *100*, 1645.
(2) Stille, J. K.; Frey, D. A. *J. Am. Chem. Soc.* 1961, 83, 1697.
(3) Gibson, H. W.; Bailey, F. C.; Epstein, A. J.; Rommelmann, H.; Pochan, J. M. J. Chem. Soc., *Chem. Commun.* 1980, 426.
(4) Gibson, H. W.; Epstein, A. J.; Rommelmann, H.; Tanner, D. B.; Yang, X.-Q.; Pochan, J. M. *J. Phys. (Paris) Colloq.* C-3 1983, *44*, 651.
(5) Gibson, H. W.; Bailey, F. C.; Epstein, A. J.; Rommelmann, H.; Kaplan, S.; Harbour, J.; Yang, X.-Q, Tanner, D. B.; Pochan, J. M. *J. Am. Chem. Soc.* 1983, *105*, 4417.
(6) Kim, Y.-H.; Gal, Y.-S.; Kim, U.-Y.; Choi, S.-K. *Macromolecules* 1988, *21*, 1991.
(7) Ryoo, M.-S.; Lee, W.-C.; Choi, S.-K. *Macromolecules* 1990, *23*, 3029.
(8) Jang, M.-S.; Kwon, S.-K.; Choi, S.-K. *Macromolecules* 1990, *23*, 4135.
(9) Koo, K.-M.; Han, S.-H.; Kang, Y.-S.; Kim, U.-Y.; Choi, S.-K. *Macromolecules* 1993, *26*, 2485.
(10) Kang, K.-L.; Kim, S.-H.; Cho, H.-N.; Choi, K.-Y.; Choi, S.-K. *Macromolecules* 1993, *26*, 4539.
(11) Kim, S.-H.; Kim. Y.-H.; Cho, H.-N.; Kwon, S.-K.; Kim, H.-K.; Choi, S.-K. *Macromolecules* 1996, *29*, 5422.
(12) Fox, H. H.; Schrock, R. R. *Organometallics* 1992, *11*, 2763.
(13) Fox, H. H.; Wolf, M. O.; O'Dell, R.; Lin, B. L.; Schrock, R. R.; Wrighton, M. S. *J. Am. Chem. Soc.* 1994, *116*, 2827.
(14) Schattenmann, F. J.; Schrock, R. R.; Davis, W. M. *J. Am. Chem. Soc.* 1996, *118*, 3295.
(15) Schattenmann, F. J.; Schrock, R. R. *Macromolecules* 1996, *29*, 8990.
(16) Schrock, R. R.; Tonzetich, Z. J.; Lichtscheidl, A. G.; Muller, P. Organometallics 2008, *27*, 3986.

(17) Krause, J. O.; Zarka, M. T.; Anders, U.; Weberskirch, R.; Nuyken, O.; Buchmeiser, M. R. Angew. Chem., Int. Ed. 2003, *42*, 5965.
(18) Koltzenburg, S.; Eder, E.; Stelzer, F.; Nuyken, O.; *Macromolecules*, 1999, *32*, 21.
(19) Krauze, J. O.; Nuyken, O.; Buchmeiser, M. R. C*hem. Eur. J.* 2004, *10*, 2029.
(20) Halbach, T. S.; Krause, J. O.; Nuyken, O.; Buchmeiser, M. R. *Macromol. Rapid. Commun*. 2005, *26*, 784.
(21) Mayershofer, M. G.; Nuyken, O.; Buchmeiser, M. R. *Macromolecules* 2006, *29*, 3484.
(22) Vygodskii, Y. S.; Shaplov, A. S.; Lozinskaya, E. I.; Vlasov, P. S.; Malyshkina, I. A.; Gavrilova, N. D.; Kumar, P. S.; Buchmeiser, M. R. *Macromolecules* 2008, *41*, 1919.
(23) Kumar, P. S.; Wurst, K.; Buchmeiser, M. R. *J. Am. Chem. Soc*. 2009, *131*, 387.
(24) Kang, E.−H.; Lee, I. S.; Choi, T.−L*. J. Am. Chem. Soc*. 2011, *133*, 11904.
(25) Kang, E.−H.; Lee, I.−H.; Choi, T.−L. *ACS Macro Lett*. 2012, *1*, 1098.
(26) Lee, I. S.; Kang, E.−H.; Park, H.; Choi, T.−L. *Chem. Sci*. 2012, *3*, 761.
(27) Park, H.; Lee, H.−K.; Choi, T.−L. *Polym. Chem.* 2013, *4*, 4676.
(28) Kim, J.; Kang, E.−H.; Choi, T.−L. *ACS Macro Lett*. 2012, *1*, 1090.
(29) Hong, S. H.; Day, M. W.; Grubbs, R. H. *J. Am. Chem. Soc*. 2004, *126*, 7414.
(30) Sudheendran, M.; Horecha, M.; Kiriy, A.; Gevorgyan, S. A.; Krebs, F. C.; Buchmeiser, M. R. *Polym. Chem*. 2013, *4*, 1590.
(31)Meldrum, A. N. A*. J. Chem. Soc.* 1908, *93*, 598.
(32) Leibfarth, F. A.; Kang, M.; Ham, M.; Kim, J.; Compos, L. M.; Gupta, N.; Moon, B.; Hawker, C. J. *Nat. Chem*. 2010, *2*, 207.
(33) Miyamura, Y.; Park, C.; Kinbara, K.; Leibfarth, F. A.; Hawker, C. J.; Aida, T. *J. Am. Chem. Soc.* 2011, *133*, 2840.

(34) Kim, J.-E.; Kang, E.-H.; Choi, T.-L. *ACS Macro Lett.* 2012, *1*, 1090-1093.
(35) Kim, K. O. ; Choi, T.-L. *Macromolecules* 2013, *46*, 5905-5914
(36) Kang,E.-H.; Lee, I.-H.; Choi, T.-L. *ACS Macro Letters* 2012, *1*, 1098
(37) Kang,E.-H.; Choi, T.-L. *ACS Macro Letters* 2013*, 2,* 780-784
(38) (a) Bassler, H.; Schweitzer, B. *Acc. Chem. Res.* 1999, *32*, 173.
(b) Heeger, A. J. *Chem. Soc. Rev.* 2010, *39*, 2354.